OXFORD

SOT | Society of Toxicology
www.toxsci.oxfordjournals.org

TOXICOLOGICAL SCIENCES, 159(1), 2017, 159–169

doi: 10.1093/toxsci/kfx121
Advance Access Publication Date: June 15, 2017
Research Article

Mechanistic Toxicity Tests Based on an Adverse Outcome Pathway Network for Hepatic Steatosis

Michelle M. Angrish, Charlene A. McQueen,[1] Elaine Cohen-Hubal, Maribel Bruno, Yue Ge, and Brian N. Chorley[2]

National Health and Environmental Effects Research Laboratory , United States Environmental Protection Agency, Research Triangle Park, North Carolina, USA

[1]Present address: Department of Pharmacology and Toxicology, University of Arizona, Tucson, AZ 85719.
[2]To whom correspondence should be addressed at U.S. Environmental Protection Agency, National Health and Environmental Effects Research Laboratory, 109 T. W. Alexander Drive, Mail Drop B-105-03, Research Triangle Park, NC 27709. Fax: 1-919-541-0694. E-mail: chorley.brian@epa.gov.

ABSTRACT

Risk assessors use liver endpoints in rodent toxicology studies to assess the safety of chemical exposures. Yet, rodent endpoints may not accurately reflect human responses. For this reason and others, human-based *in vitro* models are being developed and anchored to adverse outcome pathways to better predict adverse human health outcomes. Here, a networked adverse outcome pathway-guided selection of biology-based assays for lipid uptake, lipid efflux, fatty acid oxidation, and lipid accumulation were developed. These assays were evaluated in a metabolically competent human hepatocyte cell model (HepaRG) exposed to compounds known to cause steatosis (amiodarone, cyclosporine A, and T0901317) or activate lipid metabolism pathways (troglitazone, Wyeth-14,643, and 22(R)-hydroxycholesterol). All of the chemicals activated at least one assay, however, only T0901317 and cyclosporin A dose-dependently increased lipid accumulation. T0901317 and cyclosporin A increased fatty acid uptake, decreased lipid efflux (inferred from apolipoprotein B100 levels), and increased fatty acid synthase protein levels. Using this biologically-based evaluation of key events regulating hepatic lipid levels, we demonstrated dysregulation of compensatory pathways that normally balance hepatic lipid levels. This approach may provide biological plausibility and data needed to increase confidence in linking *in vitro*-based measurements to chemical effects on adverse human health outcomes.

Key words: adverse outcome pathway; chemical risk assessment; high-throughput toxicity testing; mechanistic toxicology; nonalcoholic fatty liver disease; hepatic steatosis.

Hepatic steatosis is a pathological condition that can lead to liver failure, altered xenobiotic metabolism (Donato *et al.*, 2006; Gomez-Lechon *et al.*, 2009), and sensitization to endocrine disruption (Berlanga *et al.*, 2014; Koo, 2013) including thyroid disease (Pacifico *et al.*, 2013). Risk assessors and regulators (Kaiser *et al.*, 2012) currently use a number of liver endpoints, including hepatic steatosis, from epidemiological and rodent toxicology studies to assess the safety of exogenous chemical exposures. Critically, rodent physiologic responses to chemical perturbation do not always reflect human responses. Differences in rodent behaviors, endocrine signaling, and metabolism confound attempts to translate findings from rodent toxicity studies to human pathophysiology (Bergen and Mersmann, 2005). Furthermore, traditional toxicity testing approaches are time and resource intensive and create a bottleneck to test the health effects of nearly 100 000 registered chemicals of unknown toxicity (Toxic Substances Control Act registry, https://www.epa.gov/tsca-inventory/how-access-tsca-inventory; last accessed June 22, 2017). For these reasons, alternative *in vitro* human cell models are being developed to accelerate the pace of the chemical evaluation process. For example, the U.S. EPA launched the Toxicity Forecaster (ToxCast) program in 2007 (Dix *et al.*, 2007). ToxCast uses high-throughput screening (HTS) and computational toxicology to evaluate large sets of chemicals for effects on a wide range of biological activity.

Table 1. Test Chemical List

Chemical	Tested [μM]	General Description	Liver Mode of Action	Citations
amiodarone hydrochloride	5.0, 15.8, 50[a]	Antiarrhymatic medication used to treat cardiac arrhythmia. Steatotic and hepatotoxic.	Possible HNF4α, PPARα, PPARγ, PXR, RXRα	Antherieu *et al.* (2011), Fromenty and Pessayre (1997), Tolosa *et al.* (2016), Vitins *et al.* (2014)
cyclosporin A	5.0, 15.8, 50	Immunosuppressant drug. Steatotic and hepatotoxic.	Oxidative Stress, mitochondrial dysfunction.	Donato *et al.* (2012), Rezzani (2006), Tolosa *et al.* (2016), Van Summeren *et al.* (2011)
T0901317	1.58, 5.0, 15.8	Upregulates genes associated with cholesterol and bile acid synthesis. Synthetic LXR agonist. Steatotic.	LXR, FXR, PXR	Grefhorst *et al.* (2002), Houck *et al.* (2004)
Troglitazone	1.0, 3.16, 10	Antidiabetic and anti-inflammatory drug removed from the market because it caused drug induced liver injury. Hepatotoxic.	PPARα and PPARγ	Chojkier (2005), Jaeschke (2007)
Wyeth-14,643	5.0, 15.8, 50	Chemical developed by the pharmaceutical industry to lower serum cholesterol. Not used clinically. Hepatotoxic.	PPARα	Larter *et al.* (2012), Woods *et al.* (2007)
22(R)hydroxycholesterol	5.0, 15.8, 50	Endogenous steroid hormone biosynthetic intermediate and LXR agonist. Has not been observed to be steatotic nor hepatotoxic.	LXR, FXR	Deng *et al.* (2006), Hessvik *et al.* (2012), Larter *et al.* (2012), Woods *et al.* (2007)

[a]Overt toxicity observed by microscopy and cytotoxicity assay.

As the *in vitro* HTS toxicity testing paradigm has evolved to address the need to rapidly evaluate large numbers of chemicals, so have evaluations to frame this data in a biologically meaningful context. An example is the adverse outcome pathway (AOP) concept, which is related to the toxicity pathway and mode-of-action paradigms for toxicological risk assessment (Ankley *et al.*, 2010). A primary driver of developing the AOP framework was to better interpret high-throughput data by connecting assay endpoints to a series of biological pathways that lead to an adverse outcome (AO) (Ankley *et al.*, 2010; Villeneuve *et al.*, 2014). We previously assembled an interconnected network of linear AOPs (ie, an AOP network) for hepatic steatosis that was characterized by 4 apical key events (KEs)—fatty acid uptake, efflux, synthesis, and oxidative metabolism (Angrish *et al.*, 2016). Hepatic steatosis is not a direct chemical-receptor mediated effect and instead results from an imbalance of these interacting biological processes. For example, hepatic fat retention could result from *both* a chemical-mediated decrease in fatty acid breakdown by disrupting mitochondrial-mediated β-oxidative metabolism *and* decreasing very low-density lipoprotein (VLDL, a carrier of fatty acid-derived triglycerides) efflux, as observed in rodent liver with carbon tetrachloride exposure (Kaiser *et al.*, 2012). Alternatively, an increase of fatty acid uptake alone, such as a transient increase in fatty acid in the blood due to a meal, may be balanced by normal responses mediated by the other compensatory mechanisms. Therefore, it may be important to evaluate the 4 KE of hepatic steatosis (fatty acid uptake, efflux, synthesis, and oxidative metabolism) to mechanistically understand the action of steatotic chemicals.

Given the large amount of scientific evidence on the mechanism, mode of action, potential serious human health impacts, and increased risk to chemical exposures associated with hepatic steatosis, we developed biologically based toxicity tests for steatotic KEs that, when unbalanced, can lead to the initiation and progression of the disease. Specifically, here we describe the development of assays for lipid uptake, lipid efflux, fatty acid oxidation (FAO), lipid accumulation, cytotoxicity, and gene expression. These assays were evaluated in the HepaRG human hepatocyte. This cell model overcomes the serious limitations of the commonly used hepatoma cell line, HepG2, that are metabolically incompetent, lack chemical transport function, and fail to adequately express transcription factors (Jackson *et al.*, 2016; Kanebratt and Andersson, 2008; Tolosa *et al.*, 2016). A defined chemical selection was used to evaluate the KE assay suite (Table 1). Three of the test chemicals had reported steatotic effects in various models: T0901317 (sulfonamide and liver X receptor [LXR] agonist), cyclosporin A (potent immunosuppressant, also a known cholestatic compound), and amiodarone (antiarrhythmic medication, also known to cause phospholipidosis in hepatocytes). Three other compounds were chosen that did not have strong evidence for hepatic steatosis effects but exhibited lipid metabolism-associated nuclear receptor activation that could perturb the test KE assays: 22(R)-hydroxycholesterol (an endogenous LXR agonist), Wyeth-14 643 (a hepatotoxic peroxisome proliferator activated receptor [PPAR] α agonist), and troglitazone (a hepatotoxic PPARγ agonist). The overall goal for developing a networked AOP-driven suite of assays for hepatic steatosis was to demonstrate a strategic *in vitro* chemical exposure evaluation by measuring KEs of compensatory pathways that, when sufficiently disrupted, could lead to an AO.

MATERIALS AND METHODS

Chemicals and reagents. Chemicals and test concentrations are listed in Table 1 and were purchased from Sigma-Aldrich (St Louis, Missouri). Oleic acid (CAS-No. 112-80-1), fatty acid free bovine serum albumin (CAS-No. 9048-46-8), Nile Red (CAS-No. 7385-67-3), and Hoechst 33342 (CAS-No. 23491-52-3) were purchased from Sigma-Aldrich. Chemical stock solutions were prepared in DMSO and diluted by serial ½ log increments. Oleic acid was dissolved in chloroform at 50 mg/ml. The fatty acid synthase (FASN,

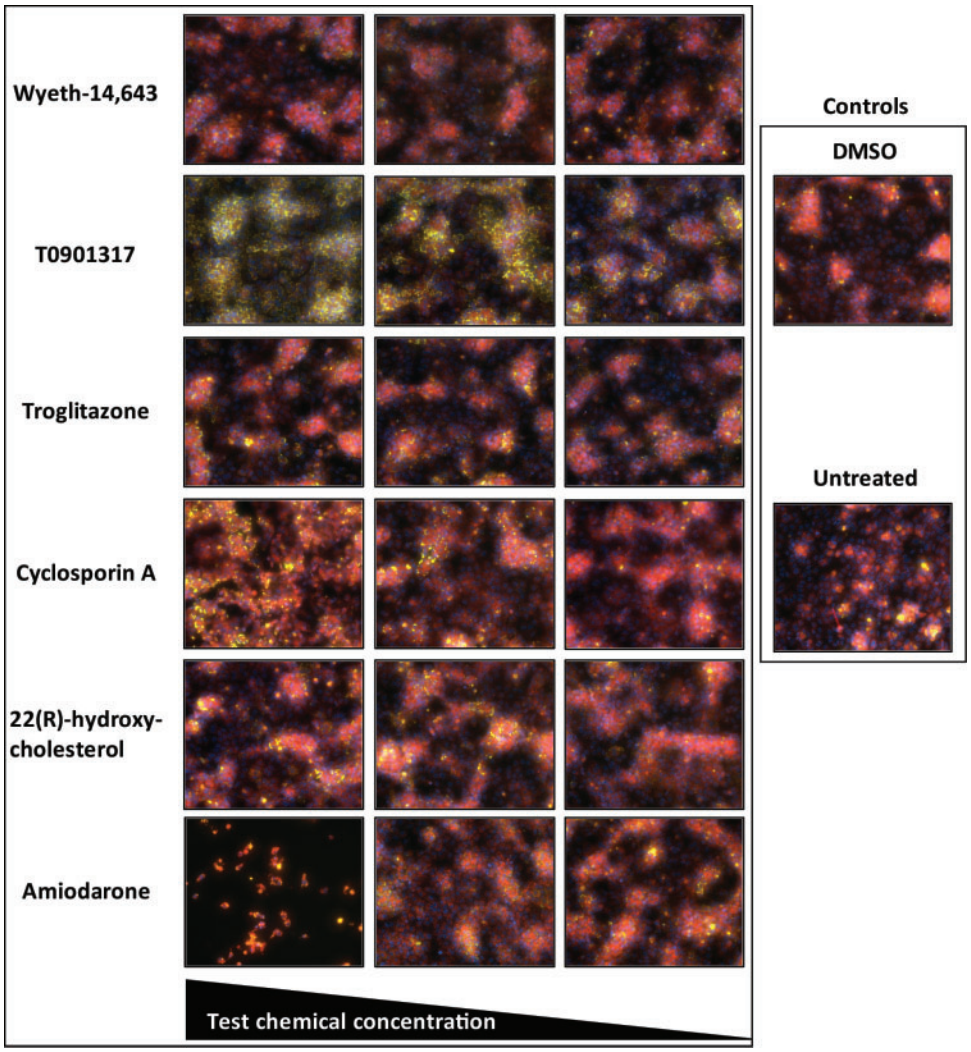

Figure 1. Representative images of HepaRG cells treated with Wyeth-14,643 (50, 15.8, 5.0 μM), T0901317 (15.8, 5.0, 1.58 μM), troglitazone (10.0, 3.16, 1.0 μM), cyclosporin A (50, 15.8, 5.0 μM), 22(R)hydroxycholesterol (50, 15.8, 5.0 μM), amiodarone (50, 15.8, 5.0 μM), DMSO, and untreated. Fluorescence of Nile Red (to selectively stain for phospholipid rich environments (red) or lipid droplets (yellow); and Hoechst 33342 to stain for nuclei (blue) are included, 20× magnification.

Cat no. 31889) and vinculin rabbit (Cat no. 13901) antibodies were purchased from Cell Signaling Technology (Beverly, MA). BCA protein Assay kit (Cat no. 232250) was purchased from Thermo Scientific (Rockford, Illinois).

Cell culture and chemical treatment. NoSpin HepaRG™ cells were purchased from Triangle Research Labs (Durham, North Carolina), thawed, suspended in thawing and plating medium (MH100 NoSpin HepaRG Base Medium and HepaRG™ Base Medium Supplement, Cat no. MH100; NoSpin HepaRG™ Media Thawing and Plating Additive, Cat no. MHTAP; Triangle Research Labs), and seeded at a density of 100 000 cells per well into 96-well black wall, clear bottom tissue culture plates. Cells were cultured at 5% CO_2, 37 °C and 85% humidity, and the medium was renewed every 48 h according to the assay conditions described below. Cells were used in the free fatty acid uptake/fatty acid efflux assays or 200 μl RNeasy Lysis Buffer (RLT) lysis buffer (Qiagen RNeasy Kit; Valencia, CA) was added to each well and the plate was stored at −80 °C until RNA isolation.

Lipid accumulation assay. On the fifth day of culture, cells were preloaded with lipid by supplementing thawing and plating media with 50 μM oleic acid conjugated to bovine serum albumin at a molar ratio of 6:1 and incubated for an additional 24 h. On the sixth day of culture, cells were treated with chemical stocks (1000×) diluted in cell culture media and incubated at 5% CO_2, 37 °C, and 85% humidity for 48 h. After treatment the medium was removed and reserved at −80 °C for lactate dehydrogenase (LDH) cytotoxicity and fatty acid efflux assays (Figure 1). Cells were washed with phosphate-buffered saline (PBS), fixed with 4% paraformaldehyde in PBS (sc-281692, Santa Cruz Biotechnology, Inc., Dallas Texas) for 20 min, and washed twice with PBS. Nile Red (1 mg/ml in methanol; to selectively stain for lipid accumulation) and Hoechst 33342 (5 mg/ml in water; to stain for nuclei as a normalization metric) were diluted 1000× in PBS. One-hundred microliters of the mixture were added to each well, and the plate was incubated for 15 min in the dark on a shaker. The plate was washed twice with 200 μl PBS. One-hundred microliters PBS were added to each well and the excitation/emission 510/580, 552/636, and 350/461 nm were measured on a CLARIOstar microplate reader (BMG Labtech, Inc., Cary, North Carolina). Data were analyzed as described below. Images were also captured using a Nikon Eclipse Ti Microscope equipped with a 20× long objective, yellow fluorescent protein (excitation 500/20 nm, DM

515 nm, emission 535/30 nm), tetramethylrhodamine (excitation 540/25 nm, emission 605/55 nm), and 4',6-diamidino-2-phenylindole (excitation 360/40 nm, emission 460-50 nm) fluorescence filter cubes, and an Andor Zyla sCMOS camera. Images were acquired under the control of NIS-Elements software (Nikon Instruments, Inc., Melville, New York).

LDH cytotoxicity assay. Cytotoxicity was evaluated by LDH cytotoxicity assay (88953, ThermoFisher Scientific, Waltham, Massachusetts) according to the manufacturer's protocol with slight modification. Cell culture medium was thawed and diluted 1:4 with plating media. Fifty microliters each of diluted test sample was mixed with 50 µl Reaction Mixture (included with kit) and incubated in the dark for 30 min. Fifty microliters of Stop solution was added to each well and the absorbance of 490 and 680 nm read on the CLARIOstar microplate reader. The background signal was removed (A490-A680) and test samples with overt cytotoxicity (see Supplementary Figure 1) were excluded from further analysis.

Fatty acid efflux assay. Fatty acid efflux was inferred from apolipoprotein B100 (APOB100) levels. APOB100 is exclusively synthesized in the liver of humans and functions as a scaffold for lipids effluxed from the liver in VLDL particles. On the day of the assay, media was thawed and APOB100 levels were measured from 1:20 diluted media by ELISA according to the manufacturer's protocol (Human Apolipoprotein B ELISA kit, Cat no. ab108807; Abcam, Cambridge, Massachusetts). Sample concentration (reported in µg/ml) was calculated from the applied standard curve and corrected for dilution. Data were analyzed as described below.

Free fatty acid uptake assay. Free fatty acid uptake assays (ab176768; Abcam, Cambridge, Massachusetts, USA) were performed according to the manufacturer's protocol with a slight modification. On the sixth day of culture, lipids were depleted for 1 h by incubating cells in completed base medium with MHIND supplement (Triangle Research Labs, LLC, Durham, North Carolina). Cells were treated with chemical stocks diluted in cell culture media and incubated at 5% CO_2, 37 °C, and 85% humidity. After 2 h of chemical treatment, cells were treated with a proprietary dodecanoic acid fluorescent fatty acid substrate (TF2-C12) in assay buffer and incubated an additional 2 h at 5% CO_2, 37 °C, and 85% humidity. The excitation/emission 485/515 nm was read on a CLARIOstar monochromator.

FAO assay. The oxygen consumption rate (OCR) due to oxidation of exogenous fatty acids was measured using a Seahorse XFe96 extracellular flux analyzer (Agilent Technologies, Santa Clara, California). HepaRG cells were suspended in thawing and plating media and seeded into collagen coated 96-well Seahorse microplates at 20 000 cells/well (identified as the optimal cell density given the cell type with Seahorse cell culture plate well size and oligomycin/ carbonyl cyanide 4-[trifluoromethoxy] phenylhydrazone [FCCP] concentrations used). Media was renewed every 48 h and after 96 h culture (24 h before the assay) lipids were depleted by renewing with substrate limited media (Dulbecco's Modified Eagle's Medium supplemented with 0.5 mM glucose, 1 mM GlutaMAX, 0.5 mM carnitine and 1% FBS, pH 7.4). Twenty-four hours later, chemicals were diluted in FAO assay media (KHB: 111 mM NaCL, 4.7 mM KCl, 1.25 mM $CaCl_2$, 2 mM $MgSO_4$, 1.2 mM NaH_2PO_4) supplemented with 2.5 mM glucose, 0.5 mM carnitine, and 5 mM HEPES on the day of the assay and adjusted to pH 7.4 at 37 °C. Cells were washed one time with the FAO assay media and 135 µl assay media was added. Cells were degassed for 45 min in a 37 °C nonCO_2 incubator. The cell assay cartridge was loaded as follows: 15 µl 10× chemical stock (15.8 µM final) or the negative control etomixir (40 µM final) into Port A, 20 µl oligomycin (3.0 µM final) into Port B, 22 µl FCCP (2.5 µM final) into Port C, and 25 µl rotenone/antimycin A (AA) mix (2 or 4 µM final, respectively) into Port D. The cartridge was loaded into the flux analyzer and calibrated. Immediately before beginning the assay, 30 µl XF Palmitate-bovine serum albumin (BSA) FAO substrate or BSA control was added to the appropriate wells. The plate was loaded into the XFe analyzer and equilibrated for 12 min. The run protocol was as follows: basal measurements, 3 repetitions of (mix 3 min, wait 0 min, measure 3 min); inject port A, 3 repetitions of (mix 3 min, wait 0 min, measure 3 min); inject port B, 3 repetitions of (mix 3 min, wait 0 min, measure 3 min); inject port C, 3 repetitions of (mix 3 min, wait 0 min, measure 3 min); inject port D, 3 repetitions of (mix 3 min, wait 0 min, measure 3 min). There were a total of 15 time points and the assay duration was 1 h and 42 min. The data were baselined to the median rotenone/AA measurement at time point (T)15 of DMSO controls and scaled from 0 to 100. The basal threshold at T6 (after chemical injection) and maximal response at T12 (after FCCP injection) were analyzed as described below with the exception that the response threshold was set at 3 (basal, T6) and 1.5 (maximal response, T12) times the baseline median absolute deviation (BMAD) of vehicle-only (DMSO) controls.

Protein studies. Total protein was extracted from HepaRG cells treated with DMSO, cyclosporin A (5, 15, and 50 µM), and T0901317 (1.58, 5, and 15.8 µM) in RIPA buffer and quantitated using the BCA protein assay kit. RIPA lysis buffer (Cat no. 040-483), Rabbit Master Kit for proteins between 66 and 440 kDa (Cat no. PS-MK20), Wes capillary immunoassay instrument, and Compass analysis software were purchased from Protein Simple (San Jose, California). Protein levels of FASN (molecular weight of 273 kDa) and vinculin (molecular weight of 124 kDa) were measured from homogenates using Wes™ instrument-based capillary nano-immunoassay (ProteinSimple) according to the manufacturer's protocol. Briefly, protein and antibody concentrations were optimized such that 0.200 and 0.075 µg/µl FASN and vinculin, respectively, and 1:50 primary antibody dilution were used in the assay. Vinculin was included as a loading control. Protein samples were heated at 95°C for 5 min and then labeled with fluorescent master mix. Labeled protein samples, primary antibodies, and other reagents included in the rabbit master kit were loaded into a plate. The plate and the accompanying 25-well capillary were inserted into the Wes™ instrument and processed for 3 h. Using the Compass analysis software, the peak area ratio of the FASN/vinculin were used to determine FASN protein levels in each sample. Data are reported as fold change (FC) relative to DMSO controls with $n = 3$.

Gene expression studies. On the fifth day of culture, cells were preloaded with lipid by supplementing thawing and plating media with 50 µM oleic acid conjugated to bovine serum albumin at a molar ratio of 6:1 and incubated for an additional 24 h. On the sixth day of culture, cells were treated with chemical stocks (1000×) diluted in cell culture media and incubated at 5% CO_2, 37 °C, and 85% humidity for 48 h. After treatment the medium was removed, 200 µl RLT lysis buffer was added, and samples were lysed by freeze thawing. An additional 150 µl RLT lysis buffer was added, and total RNA was isolated according to the manufacturer's protocol with an additional on-column DNA digestion Qiagen® RNeasy® Mini Kit. Isolated RNA was dissolved in nuclease-free water, quantitated (A_{260}), and assessed for purity by determining the A_{260}/A_{280} ratio using the NanoDrop ND-

1000 spectrophotometer (NanoDrop Technologies, Wilmington, Delaware), accepting ratios of >1.9. Quantitative reverse transcriptase PCR (RT-qPCR) of target genes was performed. Briefly, 100 ng of total RNA was reverse transcribed using iScript™ cDNA Synthesis Kit as described by the manufacturer (Bio-Rad; Hercules, California). The cDNA was used as template in a 12 μl PCR reaction containing 1× PrimePCR™SYBR® Green Assay primers and SsoAdvanced™ Universal SYBR® Green Supermix set-up using the QIAgility robotic workstation (Qiagen) for automated PCR setup. PrimePCR™SYBR® Green Assay primers included *DGAT1* (assay qHsaCID0006734), *DGAT2* (assay qHsaCED0036324), *APOB* (*APOB100*; assay qHsaCID0016796), *CD36* (assay qHsaCID0011828), *ACACA* (assay qHsaCED0038035), *PPARG* (assay qHsaCID0011718), *SREBF1* (assay qHsaCID0010452), *FASN* (assay qHsaCIP0026813), *MTTP* (assay qHsaCID009236), *PP1A* (assay qHsaCED0038620), *NRL13* (assay qHsaCID0013633), *CPT1A* (qHsaCID0023721), *GAPDH* (assay qHsaCEP0041396), *ACTB* (assay qHsaCEP0036280), *HPRT* (assay qHsaCID0016375), and *TBP* (assay qHsaCID007122). PCR reactions were performed with the CFX384 Touch™ RT PCR Detection System according to the manufacturer's protocol (Bio-Rad; Hercules, Californina). cDNAs were quantified according to the $2^{-\Delta\Delta CT}$ method (Livak and Schmittgen, 2001) and normalized to the geometric mean of *GAPDH*, *ACTB*, and *HPRT* reference genes.

Data analysis. All data were analyzed in R (R 3.1.1; R Foundation for Statistical Computing, Vienna, Austria). Fatty acid efflux, fatty acid uptake, and lipid accumulation data were normalized by setting the FC equal to the sample response over the median DMSO value. The response threshold was set at $\log_2 FC \geq 3$ times the BMAD of the vehicle-only (DMSO) controls (Judson *et al.*, 2015; Karmaus *et al.*, 2016). Supplementary Materials 1–15 contained all raw assay results and R code for analysis of this data was provided in Supplementary File 16. Data were plotted in GraphPad Prism 6 (La Jolla, California) or Microsoft Excel (Redmond, Waltham) software.

RESULTS

Cell Viability

LDH is a cytosolic enzyme that is commonly used as an indicator of cytotoxicity. Overt cytotoxicity was not observed with the chemical concentrations tested, except with 50 μM amiodarone (see Supplementary Figure 1 and Supplementary Material 6) and this concentration was not further evaluated. These results were consistent with loss of nuclear staining by Hoechst 33342 in 50 μM amiodarone treated cells (Figure 1).

Hepatocellular Lipid Accumulation

Lipid accumulation was assessed by staining fixed cells with Nile Red and observed in hepatocyte-like cells (Figure 1). Nile Red is a lipophilic dye with emission spectra that shifts toward the blue spectrum as hydrophobicity increases (Greenspan and Fowler, 1985). In the presence of cell membranes and other phospholipid rich regions Nile Red emits red fluorescence (628 nm), whereas Nile Red emits yellow fluorescence (540 nm) in triglyceride rich lipid droplets. This shift in fluorescence was clearly seen in cells exposed to T0901317 and cyslosporin A. T0901317 caused marked perinuclear lipid droplet accumulation (yellow droplets, Figure 1). Cyclosporin A caused accumulation of both triglyceride rich lipid droplets and phospholipids that displaced the nucleus (yellow and red staining, Figure 1). Lipid accumulation was not observed by other chemical treatments and significant cell death was observed with an exposure of 50 μM amiodarone (Supplementary Figure 1). Quantitative analysis revealed that T0901317 (1.58, 5, and 15.8 μM) and cyclosporin A (15.8 and 50 μM) increased lipid droplet accumulation above the response threshold in a concentration responsive manner (Figure 2A). T0901317 increased phospholipid above the response threshold only at the highest concentration (15.8 μM), and cyclosporin A increased phospholipid at 15.8 and 50 μM in a concentration-responsive manner. Although near the established thresholds, Wyeth-14 643 increased phospholipids at the highest dose, and 22-(R)-hydroxycholesterol decreased phospholipid levels at the highest and lowest concentrations tested (Figure 2B). Interestingly, 15.8 μM amiodarone induced the formation of red lipid droplets that displaced the nucleus (Figure 1). Although quantitative analysis demonstrated the effect did not exceed the response threshold, our observations were consistent with previous reports of amiodarone inducing phospholipidosis in HepaRG cells (Antherieu *et al.*, 2011).

Fatty Acid Uptake

Hepatocellular lipid accumulation depends on energy balance and, in particular, lipid flux. Therefore, the effects of the six test chemicals on hepatocellular fatty acid uptake were measured. This assay takes advantage of a bodipy labeled fatty acid that fluoresces when introduced into an intracellular environment. All chemicals tested had some effect on fatty acid uptake (Figure 2C). Specifically, Wyeth-14,643 (5, 15.8, and 50 μM), T0901317 (1.58 and 15.8 μM), cyclosporin A (5 and 15.8 μM), and 22(R)-hydroxycholesterol (15.85 and 50 μM) increased fatty acid uptake at levels exceeding, but near the response threshold. In contrast, troglitazone and amiodarone treatment decreased fatty acid uptake at the highest doses tested.

Fatty Acid Efflux

Hepatic lipids also accumulate when fatty acid efflux pathways are modified. Fatty acids primarily efflux from the liver as triglycerides attached to APOB100. APOB100 is the primary structural component of VLDL, lipid-rich particles secreted by hepatocytes into the circulation. Therefore, APOB100 levels were measured from the media to infer hepatocellular lipid efflux. Both T0901317 and cyclosporin A decreased APOB100 levels in the media of HepaRG cells (Figure 2D). This observed decrease was consistent with T0901317 and cyclosporin A induction of hepatic lipid accumulation (Figs. 1 and 2A).

Fatty Acid Oxidation

FAO is another mechanism to clear intracellular fatty acids. In hepatocytes, fatty acids are primarily broken down by mitochondrial beta-oxidative pathways that require the electron transport chain and cellular respiration (oxygen consumption) in eukaryotes. To assess this, FAO was measured using the Seahorse Mito Stress Test in the presence of the exogenous fatty acid palmitate. Media conditions were severely glucose limited and meant to favor fatty acids as the primary energy source. Etomixir inhibits carnitine palmitoyl transferase-1, an enzyme required for fatty acid transport across the mitochondrial membrane, was used as a negative control. As expected, Etomixir inhibited FAO (Figure 3). Of the chemicals evaluated, only Wyeth-14,643 (a PPARα agonist) had a median effect above the established response threshold. Although there were no treatment effects on basal respiration (Figure 3, T6), Wyeth-14,643 increased maximal mitochondrial respiration in the presence of exogenous fatty acids (Figure 3, T12).

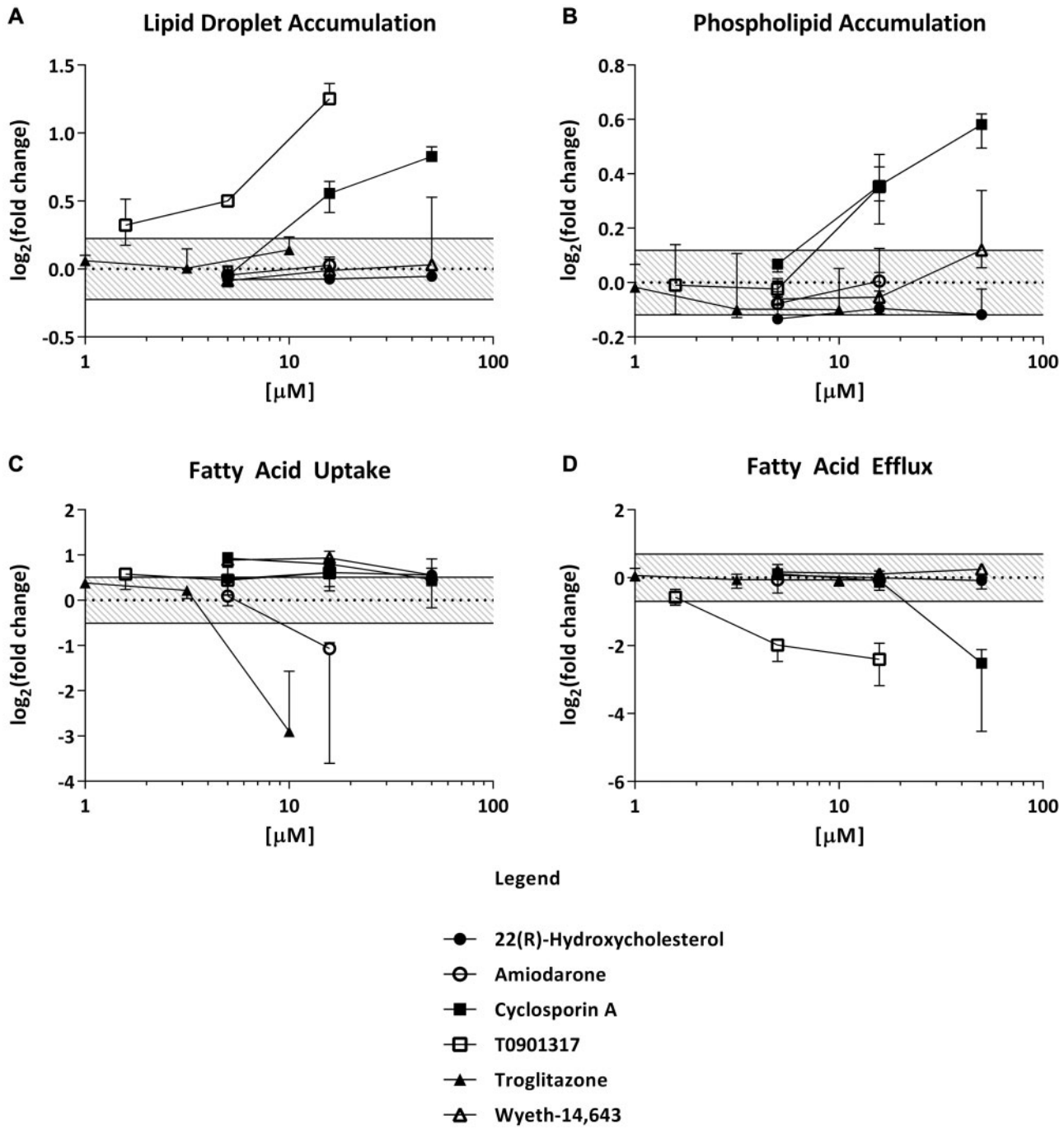

Figure 2. Key biological event assessment in HepaRG cells utilizing assays for lipid droplet accumulation (A), phospholipid accumulation (B), fatty acid uptake (C), and fatty acid efflux (D). HepaRG cells were treated for 48 hours with ½ log dilutions of 22(R)hydroxycholesterol, amiodarone, cyclosporine A, T0901317, troglitazone, Wyeth-14,643, and DMSO control. Lipid accumulation (A,B), fatty acid uptake (C), and APOB100 levels (fatty acid efflux, D) were assessed. Data are presented as the $\log_2$ FC of test samples and were considered significant for $\log_2$ FC ≥ 3 times the BMAD of DMSO controls (threshold). Bars are standard error, data points are median value, and data in the shaded region are within the threshold, reported from n = 3–4 technical replicates.

Gene Expression Analysis

Increased hepatocellular lipid levels mediated by T0901317 and cyclosporin A were consistent with increased diacylglycerol O-acyltransferase 2 mRNA levels (*DGAT2*, Table 2), an enzyme required for cellular triglyceride biosynthesis (Yen *et al.*, 2008). Consistent with troglitazone mediated decreases in fatty acid uptake, fatty acid transporter *CD36* mRNA levels were also decreased by troglitazone in a concentration dependent manner (2.3-, 8.5-, and 43.7-fold; 1.0, 3.16, and 10 μM troglitazone, respectively) compared with DMSO controls (Table 2). Interestingly, T0901317 treatment increased *APOB* mRNA levels, in contrast to decreased media APOB100 protein levels. To indirectly examine whether or not hepatic fatty acids accumulated by increased synthesis, mRNA levels of genes key to the fatty acid synthetic

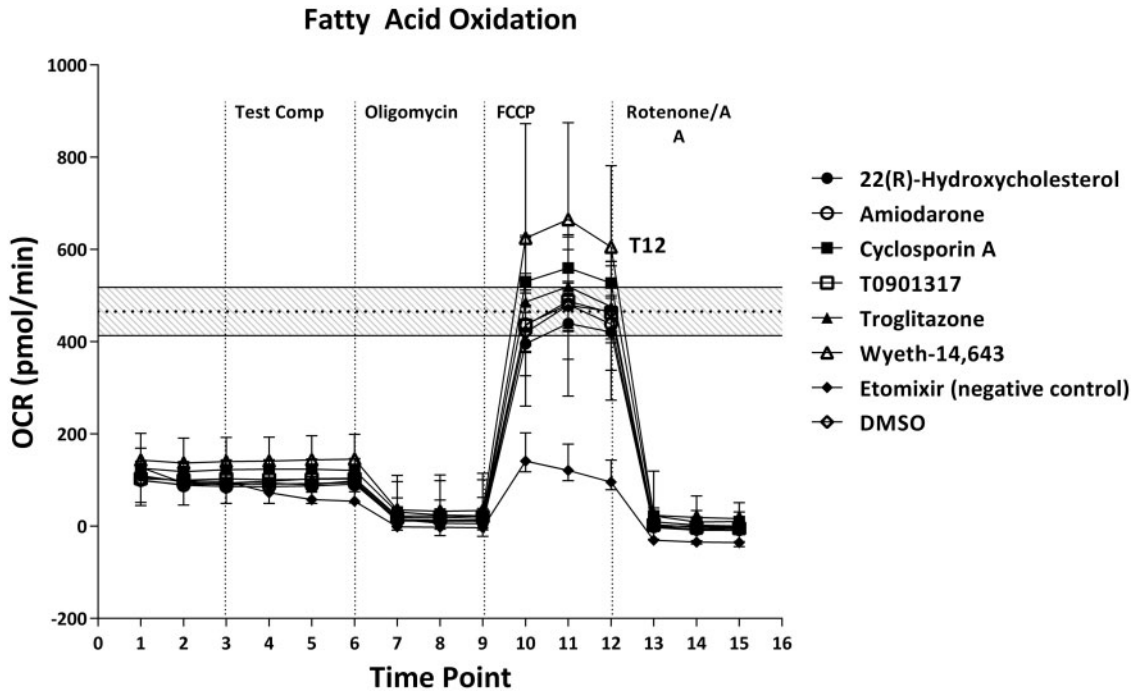

Figure 3. FAO was assessed in HepaRG cells treated with test compound (15.8 μM Wyeth-14,643, T0901317, cyclosporin A, 22(R)hydroxycholesterol, amiodarone, 10 μM troglitazone, 40 μM etomixir [negative control], and 0.01% DMSO) using the Seahorse Flux Analyzer XFe96 FAO Assay. The results are shown for chemical effects on OCR due to the oxidation of the exogenous fatty acid palmitate. Test compound, oligomycin, FCCP, and a mix of rotenone and AA were serially injected to measure chemical effects on adenosine triphosphate production, maximal respiration, and nonmitochondrial respiration. The data were baselined to the median rotenone/AA measurement at time point 15 of DMSO controls and scaled from 0 to 100. The basal threshold at T6 (after chemical injection) and maximal response at T12 (after FCCP injection) were analyzed to identify chemical effects on mitochondrial respiration outside of the response threshold (shaded region). Data reported from n = 4 technical replicates.

Table 2. Median Log_2 FC in Targeted Gene Expression Assays

		FA uptake	FA Efflux	FA Synthesis		TAG synthesis		FA oxidation	Lipid Droplet Accumulation?
Chemical	[μM]	*CD36*	*APOB*	*ACACA*	*FASN*	*DGAT1*	*DGAT2*	*CPT1A*	
T0901317	1.58	↓2.33	↑1.52	↓2.20	↓8.35	↑1.40	↑1.92		Y
	5		↑1.95	↓2.18	↓8.87	↑1.55	↑2.90	↑1.83	Y
	15.8		↑6.25	↓2.41	↓2.16	↑2.57	↑10.22	↓1.49	Y
Troglitazone	1	↓2.33							N
	3.16	↓8.53							N
	10	↓43.73	↓1.43		↓1.36	↓1.28	↓1.58		N
22(R)-Hydroxycholesterol	5	↑2.03			↑1.56		↑1.54		N
	15.8	↑3.09			↑1.74				N
	50	↑2.07			↑2.04		↑1.47		N
Cyclosporin A	5		↓1.62	↓1.60	↓1.33	↓1.36			N
	15.8		↓1.56	↓1.72			↑3.41		Y
	50				↓1.39	↑1.61	↑4.86		Y
Wyeth-14,643	5					↑1.29	↑1.46		N
	50	↓3.20					↑1.51		N
Amiodarone	15.8	↓3.20	↓1.53			↑1.37			N

↓ = FC < 3 × BMAD, ↑ = FC > 3 × BMAD, gray shading for no change; Y, yes; N, no.

process were measured. T0901317 and cyclosporin A decreased the expression of fatty acid synthesis genes *ACACA*, a rate-limiting substrate in fatty acid synthesis, and *FASN*, an enzyme that catalyzes the synthesis of fatty acids. T0901371 treatment decreased or increased the mRNA levels of *PPARG* depending on concentration and decreased sterol regulatory element binding transcription factor 1 (*SREBF1*) (Supplementary Table 1).

Protein Studies

Consistent with decreased extracellular (media) APOB100 protein measurements, intracellular APOB100 protein levels were also decreased by 1.35-fold with 15.8 μM T0901317 exposure (data not shown). These results suggested that T0901317 decreased efflux by limiting the protein scaffold (APOB100) needed to carry lipids out of the cell. This result was in contrast

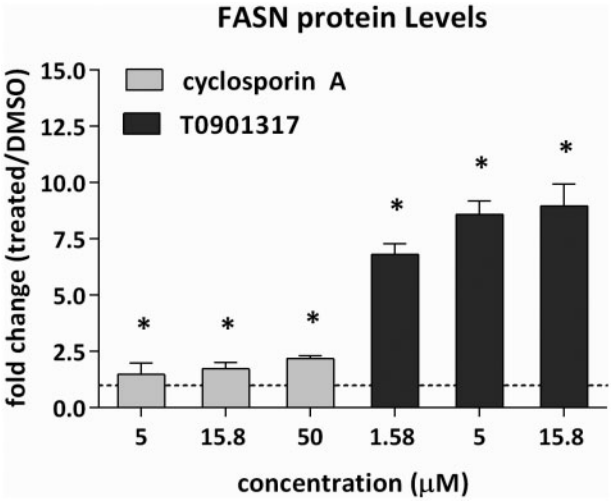

Figure 4. FASN protein levels were assessed from cyclosporin A and T0901317 treated HepaRG cell homogenate by an automated capillary immunoassay system. Bars represent FC relative to DMSO controls (dashed line). * for $p < .05$ by Mann Whitney test, n = 3.

to increased *APOB100* mRNA levels and suggested a T0901317-mediated posttranscriptional mechanism that lead to the decreased fatty acid efflux. Although fatty acid synthetic activity was not directly measured, FASN, the rate-limiting enzyme in fatty acid synthesis, was measured to infer activity. Cyclosporin A increased FASN protein levels approximately 2-fold, whereas T0901371 increased FASN protein 7- to 9-fold compared with DMSO controls (Figure 4). These results were in contrast to decreased *FASN* mRNA measurements (Supplementary Table 1) with T0901317 and cyclosporin A exposures and further supported posttranscriptional mechanisms leading to lipid accumulation.

DISCUSSION

The goal of this study was to develop and evaluate *in vitro* assays for chemical evaluation based on a networked AOP for hepatic steatosis. The data from AOP-supported assays provide biological plausibility to link *in vitro*-based measurements after chemical exposures to adverse human health outcomes. Specifically, we evaluated a suite of assays that measured KE perturbations linked to a networked AOP for hepatic steatosis (Angrish *et al.*, 2016). The underlying assumption was when biological pathways mediated by the KEs of the networked AOP were unbalanced, hepatic lipid accumulation could occur. These assays were evaluated with six compounds likely to impact these KE (lipid uptake, lipid efflux, FAO, and lipid accumulation) using an *in vitro* cryopreserved HepaRG model. The compounds were selected based on literature evidence of steatotic and/or hepatotoxic potential through various modes of action which were known to impact the KEs assessed (Table 1). The HepaRG cell line was selected as a model over other *in vitro* liver models because it was human-derived, less expensive than primary hepatocytes, less likely to include variable responses caused by inter-individual genetic differences, and maintained xenobiotic metabolism activity needed for toxicity testing (Jackson *et al.*, 2016). Of note, HepaRG cells do differentiate into a co-culture system of hepatocyte and biliary-like cells in the presence of DMSO (Cerec *et al.*, 2007). Our observations with Nile Red indicated lipid accumulation in the hepatocyte-like cells; however, we did not specifically verify cell type nor did we distinguish the specific contribution of hepatocyte or biliary-like cells to the responses measured. Furthermore, we did not assess the contribution of xenobiotic metabolism and resulting metabolites, which could have a major impact on the toxicodynamics of a chemical exposure; however, this is an area of current research in our laboratory.

Using an AOP-based targeted toxicity testing approach in a HepaRG model, we demonstrated that T0901317 and cyclosporin A caused significant lipid accumulation. These effects were mechanistically anchored using KE assays for fatty acid efflux, uptake, and synthesis. Although amiodarone treatments were previously shown to increase intracellular fatty acid levels in the HepaRG cell model (Antherieu *et al.*, 2011; Tolosa *et al.*, 2016), no significant lipid accumulation was identified after exposure in our testing conditions. These differences could be explained by both the time point evaluated and culture conditions used. Specifically, Antherieu *et al.* had not observed neutral lipid accumulation (indicated by Oil Red O stain) but noted phospholipidosis 24 h after a single exposure to 20 μM amiodarone exposure. Antherieu *et al.* observed lipid accumulation only after 14 days of repeated doses. Tolosa *et al.* measured an increase in intracellular neutral lipids 24 h after amiodarone exposure. However, Tolosa *et al.* evaluated responses after preincubation with fatty acid-free media, whereas we supplemented complete media with oleic acid 24 h prior to test chemical exposure. These differences in HepaRG culture conditions may shift the interplay between glucose and lipid metabolism that is amplified in the presence of a chemical such as amiodarone.

A key finding of this study was that hepatic steatosis was dependent on altering specific combinations of KEs above a certain threshold. For example, all 6 chemicals tested triggered activity above the established response threshold for at least one KE assay, but only 2 of those chemicals (T0901317 and cyclosporin A) induced lipid droplet accumulation in our model. This is likely explained by compensatory biological pathways that can be activated to maintain homeostasis. *In vivo*, lipid homeostasis is balanced by compensatory pathways that regulate fatty acid uptake, synthesis, efflux, and metabolism (Angrish *et al.*, 2016). This implies there is an interconnected biological network regulating lipid levels rather than a linear path. If perturbed, these alternative biological pathways may be activated. For example, even though Wyeth-14 643 increased fatty acid uptake in our HepaRG model, the observed increase in FAO likely maintained homeostasis. Likewise, multiple perturbed biological pathways may result in an AO. For T0901317 and cyclosporin A, increased uptake and decreased efflux likely tipped the balance to favor hepatic steatosis. Additionally, for T0901317, superimposing the KE assay with mRNA and protein level endpoints identified a posttranscriptional mechanism affecting APOB100 that lead to a decreased lipid efflux. These data may highlight the need for developing expert guided AOP networks, based on systems biology that can be used to scope a suite of assays that better predict the adverse effects of chemical exposures.

The steatosis AOP assays described here were developed with the premise that mechanistic and biology-based assays could add critical scientific information and data needed for the chemical evaluation process (Figure 5). Yet, the qualitative state of this AOP may limit its application to risk assessment. The chemical concentration and KE and/or AO response data could be used to estimate a benchmark dose for derivation of a point of departure (USEPA, 2012). However, the concentration-response curve created by this approach would likely model the

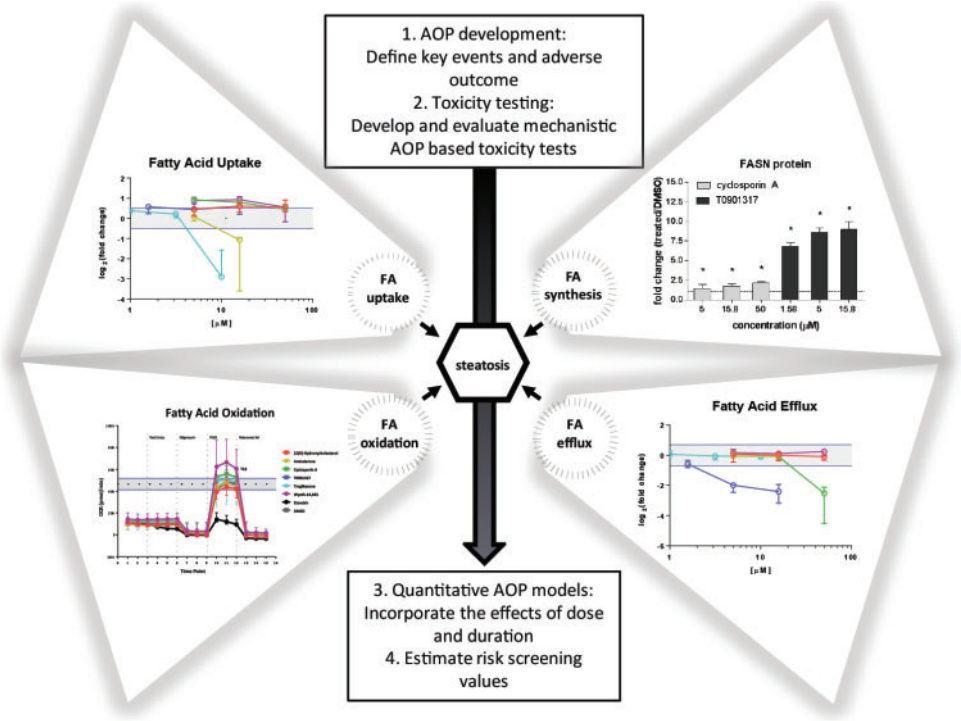

Figure 5. Summary of an AOP-based toxicity test for steatosis. An AOP network for hepatic steatosis was used to develop mechanistic toxicity tests for KEs. Leveraging scientific knowledge, mechanistic AOP-based toxicity tests, and dosimetry, the community may be able to rapidly and formally describe (with empirical data) causal relationships between exposure and health effects.

AO (lipid accumulation measured by Nile Red fluorescence) as the response implicit of the other KEs. As indicated, the "lipid accumulation" outcome is dependent on the compensatory actions of more than one KE and therefore this model would lack explicit mechanistic detail added by the other biologically based KE assays. These ideas were recently alluded to by Conolly *et al.* (2017) who described the quantitative (q)AOP concept using aromatase inhibition as a case study. To create the qAOP, the authors modeled KEs and KE relationships (defined by quantitative relationships of exposure dose and duration) *in silico*. The qAOP was then applied to an ecological risk assessment, specifically addressing chemical exposure effects on fish population dynamics. This study demonstrated how AOP networks and qAOPs (driven by mechanistic and biological-based data) can use *in vitro* data and reduce overall uncertainty in the chemical risk assessment process.

AOP networks are a critical step toward improving the weight of evidence for chemical hazard characterization. In the past decade, high-throughput *in vitro* evaluation of "toxicity pathways", defined as "pathways that can lead to adverse health effects when sufficiently perturbed" (Rainham *et al.*, 2010), and more recently linear AOPs (https://aopwiki.org/, accessed 06/22/17), have been useful prioritization tools. In order to evaluate chemical impacts on human health, however, these AOPs and toxicity pathways need to be networked to more clearly represent complex biological and ecological systems. For example, selective chemicals (ie, mediated by nuclear receptor activation) may lead to pleiotropic effects too far upstream of an apical endpoint to causally anchor that specific event to an AO. Therefore, a single *in vitro* assay may accurately predict chemical-mediated proximal effects directly dependent on receptor activation; however, this assay could fail to predict responses dependent on compensatory, adaptive, feedback, and other related mechanisms that ultimately impact apical KEs. AOP networks may help reduce the uncertainty in those predictions by using interconnected KEs or "biological landmarks" (such as lipid efflux and uptake) that can be causally linked to an AO. The utility of this approach is that a suite of biologically based assays can also provide the science-based analysis and data needed to predict responses from chemicals that act through less selective molecular interactions (Thomas *et al.*, 2013). For example, LXR activation or changes in *APOB* mRNA levels by T0901317 alone are not sufficient evidence to infer hepatic steatosis. However, effects on LXR and *APOB* in combination with impaired lipid efflux and increased lipid uptake provides better mechanistic evidence to anchor T0901317 exposure to lipid accumulation. This is a critical concept in the evolution of predictive toxicology; by integrating expert opinion, experimental evidence, and AOPs, it is possible to organize massive data sets into groups or "AOP fingerprints" predictive of downstream KEs.

By design, AOP networks can be leveraged as guidance tools to organize chemical evaluation data that already exists to assess chemical risk for endpoints of regulatory concern. Rapid and defensible chemical assessment methods are necessary to evaluate the potential health hazards of the tens of thousands chemicals in commerce and the environment. The approach described in this study demonstrates the value of applying a biologically based framework to evaluate important endpoints. AOP-based testing batteries can be applied to both prioritize chemical evaluation and predict potential for human health and ecological adversity.

SUPPLEMENTARY DATA

Supplementary data are available at *Toxicological Sciences* online.

ACKNOWLEDGMENTS

We would like to thank Dr Steve Simmons and Danielle Suarez for their help with assay development and analysis; Dr Steve Ferguson and Dr Sreenivasa Ramaiahgari for help with HepaRG culture; Dr Eric Watt for guidance analyzing the data; and Dr Phillip Kaiser, Dr Chad Deisenroth, and Ms Michelle Campbell for their reviews of this article.

FUNDING

Funding for this study came from the U.S. Environmental Protection Agency Office of Research and Development. The research described in this article has been reviewed by the National Health and Environmental Research Laboratory of U.S. Environmental Protection Agency and approved for publication. Approval does not signify that the contents necessarily reflect the views and the policies of the Agency. Mention of trade names or commercial products does not constitute endorsement or recommendation for use.

REFERENCES

Angrish, M. M., Kaiser, J. P., McQueen, C. A., and Chorley, B. N. (2016). Tipping the balance: Hepatotoxicity and the 4 apical key events of hepatic steatosis. *Toxicol. Sci.* **150**, 261–268.

Ankley, G. T., Bennett, R. S., Erickson, R. J., Hoff, D. J., Hornung, M. W., Johnson, R. D., Mount, D. R., Nichols, J. W., Russom, C. L., Schmieder, P. K., *et al.* (2010). Adverse outcome pathways: A conceptual framework to support ecotoxicology research and risk assessment. *Environ. Toxicol. Chem.* **29**, 730–741.

Antherieu, S., Rogue, A., Fromenty, B., Guillouzo, A., and Robin, M. A. (2011). Induction of vesicular steatosis by amiodarone and tetracycline is associated with up-regulation of lipogenic genes in HepaRG cells. *Hepatology* **53**, 1895–1905.

Bergen, W. G., and Mersmann, H. J. (2005). Comparative aspects of lipid metabolism: Impact on contemporary research and use of animal models. *J. Nutr.* **135**, 2499–2502.

Berlanga, A., Guiu-Jurado, E., Porras, J. A., and Auguet, T. (2014). Molecular pathways in non-alcoholic fatty liver disease. *Clin. Exp. Gastroenterol.* **7**, 221–239.

Cerec, V., Glaise, D., Garnier, D., Morosan, S., Turlin, B., Drenou, B., Gripon, P., Kremsdorf, D., Guguen-Guillouzo, C., and Corlu, A. (2007). Transdifferentiation of hepatocyte-like cells from the human hepatoma HepaRG cell line through bipotent progenitor. *Hepatology* **45**, 957–967.

Chojkier, M. (2005). Troglitazone and liver injury: In search of answers. *Hepatology* **41**, 237–246.

Conolly, R. B., Ankley, G. T., Cheng, W., Mayo, M. L., Miller, D. H., Perkins, E. J., Villeneuve, D. L., and Watanabe, K. H. (2017). Quantitative Adverse Outcome Pathways and Their Application to Predictive Toxicology. *Environ. Sci. Technol.* **51**, 4661–4672.

Deng, R., Yang, D., Yang, J., and Yan, B. (2006). Oxysterol 22(R)-hydroxycholesterol induces the expression of the bile salt export pump through nuclear receptor farsenoid X receptor but not liver X receptor. *J. Pharmacol. Exp. Ther.* **317**, 317–325.

Dix, D. J., Houck, K. A., Martin, M. T., Richard, A. M., Setzer, R. W., and Kavlock, R. J. (2007). The ToxCast program for prioritizing toxicity testing of environmental chemicals. *Toxicol. Sci.* **95**, 5–12.

Donato, M. T., Lahoz, A., Jimenez, N., Perez, G., Serralta, A., Mir, J., Castell, J. V., and Gomez-Lechon, M. J. (2006). Potential impact of steatosis on cytochrome P450 enzymes of human hepatocytes isolated from fatty liver grafts. *Drug Metab. Dispos.* **34**, 1556–1562.

Donato, M. T., Tolosa, L., Jimenez, N., Castell, J. V., and Gomez-Lechon, M. J. (2012). High-content imaging technology for the evaluation of drug-induced steatosis using a multiparametric cell-based assay. *J. Biomol. Screen.* **17**, 394–400.

Fromenty, B., and Pessayre, D. (1997). Impaired mitochondrial function in microvesicular steatosis. Effects of drugs, ethanol, hormones and cytokines. *J. Hepatol.* **26(Suppl 2)**, 43–53.

Gomez-Lechon, M. J., Jover, R., and Donato, M. T. (2009). Cytochrome p450 and steatosis. *Curr. Drug Metab.* **10**, 692–699.

Greenspan, P., and Fowler, S. D. (1985). Spectrofluorometric studies of the lipid probe, nile red. *J. Lipid Res.* **26**, 781–789.

Grefhorst, A., Elzinga, B. M., Voshol, P. J., Plosch, T., Kok, T., Bloks, V. W., van der Sluijs, F. H., Havekes, L. M., Romijn, J. A., Verkade, H. J., *et al.* (2002). Stimulation of lipogenesis by pharmacological activation of the liver X receptor leads to production of large, triglyceride-rich very low density lipoprotein particles. *J. Biol. Chem.* **277**, 34182–34190.

Hessvik, N. P., Bakke, S. S., Smith, R., Ravna, A. W., Sylte, I., Rustan, A. C., Thoresen, G. H., and Kase, E. T. (2012). The liver X receptor modulator 22(S)-hydroxycholesterol exerts cell-type specific effects on lipid and glucose metabolism. *J. Steroid Biochem. Mol. Biol.* **128**, 154–164.

Houck, K. A., Borchert, K. M., Hepler, C. D., Thomas, J. S., Bramlett, K. S., Michael, L. F., and Burris, T. P. (2004). T0901317 is a dual LXR/FXR agonist. *Mol Genet Metab* **83**, 184–187.

Jackson, J. P., Li, L., Chamberlain, E. D., Wang, H., and Ferguson, S. S. (2016). Contextualizing hepatocyte functionality of cryopreserved HepaRG cell cultures. *Drug Metab. Dispos.* **44**, 1463–1479.

Jaeschke, H. (2007). Troglitazone hepatotoxicity: Are we getting closer to understanding idiosyncratic liver injury? *Toxicol. Sci.* **97**, 1–3.

Judson, R. S., Magpantay, F. M., Chickarmane, V., Haskell, C., Tania, N., Taylor, J., Xia, M., Huang, R., Rotroff, D. M., Filer, D. L., *et al.* (2015). Integrated model of chemical perturbations of a biological pathway using 18 in vitro high-throughput screening assays for the estrogen receptor. *Toxicol. Sci.* **148**, 137–154.

Kaiser, J. P., Lipscomb, J. C., and Wesselkamper, S. C. (2012). Putative mechanisms of environmental chemical-induced steatosis. *Int. J. Toxicol.* **31**, 551–563.

Kanebratt, K. P., and Andersson, T. B. (2008). Evaluation of HepaRG cells as an in vitro model for human drug metabolism studies. *Drug Metab. Dispos.* **36**, 1444–1452.

Karmaus, A. L., Toole, C. M., Filer, D. L., Lewis, K. C., and Martin, M. T. (2016). High-throughput screening of chemical effects on steroidogenesis using H295R human adrenocortical carcinoma cells. *Toxicol. Sci.* **150**, 323–332.

Koo, S. H. (2013). Nonalcoholic fatty liver disease: Molecular mechanisms for the hepatic steatosis. *Clin. Mol. Hepatol.* **19**, 210–215.

Larter, C. Z., Yeh, M. M., Van Rooyen, D. M., Brooling, J., Ghatora, K., and Farrell, G. C. (2012). Peroxisome proliferator-activated receptor-alpha agonist, Wy 14,643, improves metabolic indices, steatosis and ballooning in diabetic mice with non-alcoholic steatohepatitis. *J. Gastroenterol. Hepatol.* **27**, 341–350.

Livak, K. J., and Schmittgen, T. D. (2001). Analysis of relative gene expression data using real-time quantitative PCR and the 2(-Delta Delta C(T)) Method. *Methods* **25**, 402–408.

Pacifico, L., Bonci, E., Ferraro, F., Andreoli, G., Bascetta, S., and Chiesa, C. (2013). Hepatic steatosis and thyroid function tests in overweight and obese children. *Int. J. Endocrinol.* **2013**, 381014.

Rainham, D., McDowell, I., Krewski, D., and Sawada, M. (2010). Conceptualizing the healthscape: Contributions of time geography, location technologies and spatial ecology to place and health research. *Soc. Sci. Med.* **70**, 668–676.

Rezzani, R. (2006). Exploring cyclosporine A-side effects and the protective role-played by antioxidants: The morphological and immunohistochemical studies. *Histol. Histopathol.* **21**, 301–316.

Thomas, R. S., Philbert, M. A., Auerbach, S. S., Wetmore, B. A., Devito, M. J., Cote, I., Rowlands, J. C., Whelan, M. P., Hays, S. M., Andersen, M. E., *et al.* (2013). Incorporating new technologies into toxicity testing and risk assessment: Moving from 21st century vision to a data-driven framework. *Toxicol. Sci.* **136**, 4–18.

Tolosa, L., Gomez-Lechon, M. J., Jimenez, N., Hervas, D., Jover, R., and Donato, M. T. (2016). Advantageous use of HepaRG cells for the screening and mechanistic study of drug-induced steatosis. *Toxicol. Appl. Pharmacol.* **302**, 1–9.

684 USEPA (2012). *Benchmark Dose Technical Guidance*. In (Forum R. A., Ed.). 684 USEPA, Washington, DC.

Van Summeren, A., Renes, J., Bouwman, F. G., Noben, J. P., van Delft, J. H., Kleinjans, J. C., and Mariman, E. C. (2011). Proteomics investigations of drug-induced hepatotoxicity in HepG2 cells. *Toxicol. Sci.* **120**, 109–122.

Villeneuve, D. L., Crump, D., Garcia-Reyero, N., Hecker, M., Hutchinson, T. H., LaLone, C. A., Landesmann, B., Lettieri, T., Munn, S., Nepelska, M., *et al.* (2014). Adverse outcome pathway (AOP) development I: Strategies and principles. *Toxicol. Sci.* **142**, 312–320.

Vitins, A. P., Kienhuis, A. S., Speksnijder, E. N., Roodbergen, M., Luijten, M., and van der Ven, L. T. (2014). Mechanisms of amiodarone and valproic acid induced liver steatosis in mouse in vivo act as a template for other hepatotoxicity models. *Arch. Toxicol.* **88**, 1573–1588.

Woods, C. G., Burns, A. M., Bradford, B. U., Ross, P. K., Kosyk, O., Swenberg, J. A., Cunningham, M. L., and Rusyn, I. (2007). WY-14,643 induced cell proliferation and oxidative stress in mouse liver are independent of NADPH oxidase. *Toxicol. Sci.* **98**, 366–374.

Yen, C. L., Stone, S. J., Koliwad, S., Harris, C., and Farese, R. V. Jr. (2008). Thematic review series: Glycerolipids. DGAT enzymes and triacylglycerol biosynthesis. *J. Lipid Res.* **49**, 2283–2301.